On the measurement of piezoelectric d$_{33}$ coefficient of soft thin films under weak mechanical loads: A rapid and affordable method

Gaia de Marzo [a,1,*], Luca Fachechi [a,1,*], Valentina Antonaci [a,b],
Vincenzo Mariano Mastronardi [a,b], Luigi Portaluri [a,b], Maria Teresa Todaro [a,c], Luciana Algieri [b],
Antonio Qualtieri [a], Francesco Rizzi [a], Michele Scaraggi [a,b,d], Massimo De Vittorio [a,b]

[a] Center for Biomolecular Nanotechnologies, Istituto Italiano di Tecnologia, Arnesano, LE 73010, Italy
[b] Department of Engineering for Innovation, University of Salento, Lecce 73100, Italy
[c] Institute of Nanotechnology, Consiglio Nazionale delle Ricerche, Lecce 73100, Italy
[d] Department of Mechanical Engineering, Imperial College, London SW7 2AZ, UK

ARTICLE INFO

ABSTRACT

Thanks to their intrinsic flexibility, energy efficiency and high portability, soft piezoelectric thin films represent the most effective technological approach for wearable devices to monitor health conditions. In order to improve effectiveness and applicability, more and more innovative and high-performing soft piezoelectric materials are being developed and benchmarked through their piezoelectric d$_{33}$ coefficient. However, most existing methods to measure the d$_{33}$ were developed for ceramic or bulk materials and cannot be applied to soft materials because high force/pressure can deform and damage the material structure. This work introduces a simple, effective, and fast method to accurately measure the d$_{33}$ of soft and thin piezoelectric films by applying weak sinusoidal forces to avoid any damage to the sample, and simultaneously measuring the charges produced by the direct piezo-electric effect. The approach is versatile as it can be used for different types of materials and sizes of the active area. This method represents an effective solution to speed up the process of material optimization, paving the way for the rapid development of novel wearable piezoelectric devices.

1. Introduction

By virtue of their small size and portability, Micro Electro-Mechanical Systems (MEMS) have revolutionized the world of wearable devices for biomedical applications to monitor health parameters. Piezoelectric soft and flexible materials play an important role in this context thanks to their significantly improved wearability, compliance to the skin and reduced invasiveness and intrusiveness. Their main advantages are represented by their sensitivity, light weight, flexibility, possibility of being processed under different forms (thin film, fibers, sponge), and self-powering.[1–5] Thin film ceramics, like Aluminium Nitride (AlN) and Zinc Oxide (ZnO), and synthetic polymers, such as Polyvinylidene Fluoride (PVDF) and their copolymers, represent the current benchmark for flexible and biocompatible piezoelectric materials. Besides, the promising category of bioderived polymeric piezoelectric materials is attracting a growing interest thanks to their intrinsic

biocompatibility and low environmental impact, which could help reduce the amount of electronic waste produced yearly.[6] Consequently, numerous research groups are looking for strategies to improve the performances of such materials and enable the development of sensors for detecting and monitoring very light stimuli in the range of mN, such as blood pressure, breath pace and heartbeat.[7–9] The choice of an appropriate approach to increase the performance is crucial due to the strong impact that it will have on the design of the final architecture of the developed device. Commonly, this can be achieved by an iterative stream in which a new material fabrication approach is optimized, the final design of the device is tested and, if not adequate, a new fabrication and a new design are developed and so on. Therefore, to guarantee a smooth flow between the material optimization and the device's design, it is necessary to own instruments that are able to examine the performance of the piezoelectric device routinely and quickly. The piezoelectric d$_{33}$ coefficient, which quantifies the amount of charge generated

across the film thickness upon applying normal stress, is one of the main piezoelectric parameters investigated in literature to benchmark the performances of different materials. Several methods were established so far to measure the d_{33} coefficient; however, most of them were typically developed and optimized for ceramic and stiff piezoelectric materials. Consequently, the advancements in fabricating innovative devices and transducers with soft and flexible materials are progressing faster than the improvements in measuring methods, forcing researchers to adapt to inappropriate, time-consuming, and complex measurements. In particular, the most common methods apply forces in the range of N, turning out to stresses above the structural integrity limits of the soft materials. For example, the frequency method is an empiric technique based on the measurement of the impedance of the material at its resonance frequency.[10] To process this information and obtain the piezoelectric coefficient, it is necessary to measure bulk samples characterized by different geometries and extract the complete matrix of piezoelectric coefficients. However, thick samples cannot always be fabricated out of thin film materials, as well as bulk piezoelectric coefficients might easily differ from the thin film case. Alternative methods exploit the indirect or direct piezoelectric effect. In indirect methods, Laser Interferometry (LI) and Laser Scanning Vibrometry are used to record displacement while applying a voltage to the material.[11,12] The method is highly accurate and reproducible but presents some drawbacks: it requires an expensive interferometer or vibrometer equipment, suffers from environmental noise and requires an extremely flat surface with high reflectance. Furthermore, this method is not appropriate for porous materials, and the results obtained can be altered by the geometry of the sample or the charge accumulation at the edges of the electrodes. Another type of method that exploits the indirect piezoelectric effect is Piezoresponse Force Microscopy (PFM). [13–15], a potent technique to qualitatively and quantitatively measure the piezoelectric properties of thin films at the nanoscale. It involves the application of an oscillating electric field by a conductive cantilever tip in contact with the sample surface. Because of the reverse piezoelectric effect, the applied voltage induces a deformation of the material, causing the displacement of the conductive cantilever tip. The displacement can be detected and demodulated by a lock-in amplifier, directly and precisely measuring the induced substrate expansion and contraction with pm resolution deformation, similar to atomic force microscopy. PFM represents one of the most accurate methods to extrapolate the effective d_{33} coefficient. The obtained images of piezoelectric amplitude and phase accurately depict each piezoelectric domain, delivering important morphological and electrical information at the nanoscale. Nevertheless, some limitations characterize this technique. First, the substrate must be completely flat, electrostatic contributions on the tip must be negligible to not alter the measurement and, when measuring soft materials, they must be thin enough to avoid mechanical damping. Additionally, PFM, operating at the nanometric scale, focuses on the local piezoresponse contribution, leading to drastically increased measurement time when scanning a relatively large sample area. Moreover, when measuring composite materials with randomly dispersed nanosized elements, although it is possible to discriminate the contribution of each element, the effective behavior of the composite material remains undisclosed. Finally, to extrapolate the d_{33} piezoelectric coefficient, several spectra and images must be collected and carefully interpreted according to a long and complex procedure. For these reasons, while PFM is excellent for probing piezoelectric materials, it cannot be easily employed for routine and fast sample measurements at a macroscopic application length scale. Besides, other methods exploit the direct piezoelectric effect by applying a mechanical action and collecting the charges generated by the device. The so-called direct methods are fast and accurate, representing the ideal choice for routine characterization of the piezoelectric behavior of samples. Recently, pneumatic methods were developed exploiting air guns to exert controlled air stream pulses on the film surface or pressurized chambers to apply pressure by gas compression and decompression.[16,17] Whilst on one side these methods rely on a facile procedure and setup, on the other side applying impulsive loads, although feasible for ceramic materials, might easily induce nonlinear (high order) piezoelectric response in soft films, thus increasing the dispersion of the measured values. Furthermore, these methods require time to perform repeated measurements for a correct averaging of the signal. A solution to this issue was presented by the group of Ravikumar, who introduced a direct method based on ultrasonic pulses.[18] This results in a precise and non-destructive technique that ensures proper pressure application, avoiding damage to soft samples. However, the necessity of using liquids or oils to couple the ultrasound transducer and the sample hinders the possibility of employing the systems with absorbing materials, like piezoelectric hydrogel, porous materials or biopolymeric films. The Berlincourt method is the most straightforward and easy-to-apply direct method. [10,12,19] It exploits the application of an oscillating force on the sample by a couple of rounded electrodes and measures the generated charges. Thanks to its simplicity, many commercial systems were developed based on this method. Nevertheless, it was intended and suited for bulk ceramic samples and, therefore, when applied to soft and thin materials, it might introduce bias stress in the film, damaging them and potentially overestimating the d_{33} coefficient. Considering homogeneous samples, the round-shaped electrodes measure the piezoelectric response only at single points. However, polymeric thin films are less regular than ceramics, impeding the possibility of inferring the piezoelectric behavior of the entire sample. Some commercial dedicated tools were developed for soft samples with the pre-load and the applied forces in the range between one N and tens of N. Nonetheless, this range may easily result in too high pressures for soft thin films developed to work in the mN range, leading to irreversible compression and damage of the material and artifacts. Guo et al. developed a system with the help of a miniaturized hammer that requires the use of finite element method (FEM) analysis to compensate for substrate deformation, but this approach is not always feasible with innovative and unknown materials [20].

Therefore, by reviewing the existing literature, the need emerges to develop a fast and effective tool for quantifying the piezoelectric effect with sub-N forces compatible with soft materials and highly sensitive devices.[7,8] This work presents a rapid, quasi-static and intrinsically non-destructive method to measure the d_{33} coefficient of thin and soft piezoelectric films by using weak forces, thus avoiding any damage or undesired strain on the sample. The method is based on the use of a flat speaker that applies weak sinusoidal stimuli of the order of a few mN along the normal direction to the sample surfaces (z-axis), a load cell to monitor in real-time the force acting on the sample and a custom-made charge amplifier to measure the output generated by the sample under compression. The setup is also equipped with a Faraday cage to eliminate any environmental and triboelectric charge contribution.[21] The simultaneous measurement of charge and force allows extrapolating the d_{33} coefficient with values in good agreement with comparative measurements performed by the local piezoelectric response of PFM. The devices under test consisted of a piezoelectric film, with thickness spanning from 1 μm up to 15 μm, embedded between top and bottom electrodes to extract the charges generated along the normal axis in compression mode. Thanks to its mechanical and electrical design, specifically tailored for thin and flexible film, this setup enables to overcome the limitations of the above-mentioned methods, reported also in Table 1, providing a pioneering instrument to unleash the potential of innovative materials whose inspection was impeded so far by common d_{33} analysis methods. In particular, this system enables fast and accurate characterization of soft and flexible piezoelectric materials and devices, at the application length scale, supporting the quick design and development of novel devices for energy, piezocatalysis and biomedical applications.

Table 1

Comparison of the different features of the common d_{33} measurement methods, both direct and indirect, and the method proposed in this study with a particular focus on the disadvantages.

Method	Type	Non-destructive forces (only for direct method)	Precision	Scale	Time for experiment and measurements	Cost	Disadvantages	Ref.
Frequency method	indirect	Not applicable	2 %	mm	–	€	Not suitable for thin film	[10]
Laser interferometry	indirect	Not applicable	2 %	μm	hours	€€€	Environmental vibrations, optical-grade fabrication	[11,12]
PFM	indirect	Not applicable	1,5%	nm	hours/days	€€€	Specific fabrication, local measurement, electrostatic contribution	[13,14,15]
Pneumatic	direct	∼ 6N	3 %	mm	–	€	Non-linear contribution on soft samples	[16,17]
Ultrasonic	direct	–	–	mm	–	€€	Liquid necessary to couple ultrasound	[18]
Berlincourt	direct	1–10 N	4 %	mm	minutes	€	Film bending	[10,12,19]
Weak loads method	direct	5–30 mN	5 %	mm	minutes	€	Few minutes of signal stabilization	This work

2. Materials and methods

2.1. Sample preparation

Sensors were micro-fabricated using different thin-film piezoelectric materials with known properties to quantify the accuracy of the proposed set-up in the fast measurement of the piezoelectric d_{33} coefficient. PVDF sensors were fabricated from a 16 μm-thick commercial PVDF film (β phase) with both surfaces covered by 50 nm of sputtered aluminum and characterized by a $d_{33} > 18$ pC N^{-1} (PolyK) (Fig. 1**a**). To produce the sensors, top and bottom electrodes were shaped by wet etching with NaOH 1 M solution using a Kapton hard mask to obtain an active area of 8 x 8 mm^2. Then, conductive tape was used to attach the device to a board for electrical connection. Finally, the sensor was conformally covered with a 1 μm layer of Parylene-C, making it electrically isolated.

Additionally, AlN sensors were fabricated according to the protocol described elsewhere (Fig. 1**b**).[22] Briefly, a 25 μm thick Kapton (Kapton HN) foil attached with Polydimethylsiloxane (Sylgard 184) to a silicon wafer was used as the substrate to sputter, sequentially, a layer of 120 nm thick AlN, a 130 nm thick Mo bottom electrode, a 900 nm thick piezoelectric AlN layer and a 210 nm thick top Mo electrode. Then, photolithography and dry etching were employed to shape the top, piezoelectric and bottom layers. The device is then connected to a board and conformally covered with 1 μm of Parylene-C for electrical isolation.

Finally, chitosan sensors were fabricated according to the protocol described in the literature (Fig. 1**c**).[23] Briefly, 1 % w/v chitosan powder (890000 avg., Glentham) was dissolved in an aqueous solution with 1 % v/v of Lactic Acid (Sigma Aldrich) and then solvent cast overnight at 40 °C. Then, it is neutralized for 60 min with NaOH 1 M, washed and deposited on the bottom electrode of 1 μm of silver ink printed on glass (Nano Dimension). After drying, the chitosan piezoelectric film with a thickness of 15 μm is peeled off the glass and the top gold electrode 100 nm thick is fabricated by e-beam evaporation through a Kapton shadow mask. Then, the device is attached to a board by conductive tape and conformally covered with a 1 μm thick layer of Parylene-C.

Samples for PFM measurements were prepared by depositing the piezoelectric layer on a conductive and flat bottom electrode: molybdenum on silicon substrate was used for AlN, and PEDOT:PSS on glass was used for the chitosan due to its conductivity and high affinity for the material.

2.2. Measurement setup

Fig. 2**a** shows the schematic of the custom setup built to measure the d_{33} parameter. The Device Under Test (DUT) is composed of a rectangular-shaped and uniform-thickness layer of the material under testing, sandwiched between two metallic layers defining a smaller active area, as described in "sample preparation" section. The DUT is placed over a flat support mounted on the top of a load cell and a flat exciting transducer is positioned above it. Both the support and the transducer have flat surfaces in contact with the two sides of the sample, to ensure uniform distribution of contact stresses all over the surface. In particular, the electromagnetic speaker used as the actuator has a flat cover welded on the moving coil to allow, at low driving voltage, bigger displacement with relatively small loads if compared with a standard piezoelectric ceramic transducer. A thin flexible steel bar with a low spring constant exerts a pre-load on the speaker over the sample through a nylon screw. Thus, the measurement setup is stacked under load constraint, with pre-load spring stiffness much lower than the load cell spring stiffness. On one side, this ensures the stack to dynamically operate under fully compressive loads, without the occurrence of impulsive stimuli possibly resulting from contact losses. On the other side, the lower bar spring constant (with respect to the load cell) allows the pre-load to be kept almost constant during the operation of the soft actuator, targeting linearity between input actuator voltage and DUT compressive load. Furthermore, the load cell is mounted over an XY micrometric stage for fine alignment, whereas the steel bar is mounted to a Z micrometric stage to fine-tune the compression force. All metallic parts are connected to the ground and the whole setup is enclosed in a grounded Faraday cage to minimize electromagnetic interference. The setup is mounted on an anti-vibration table.

Finally, since the few grams mass of the DUT and its flat support do not quantitatively affect the resonance frequency of the load cell, the
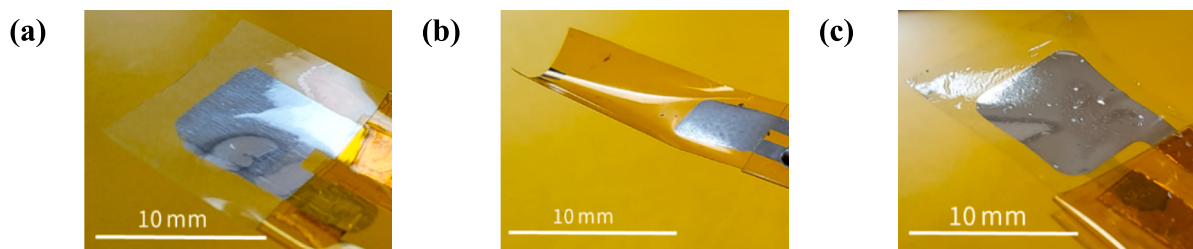

Fig. 1. A) PVDF sensor with aluminum electrodes. b) AlN sensor on kapton with molybdenum electrodes. c) Chitosan sensor with a gold top and silver bottom electrode.
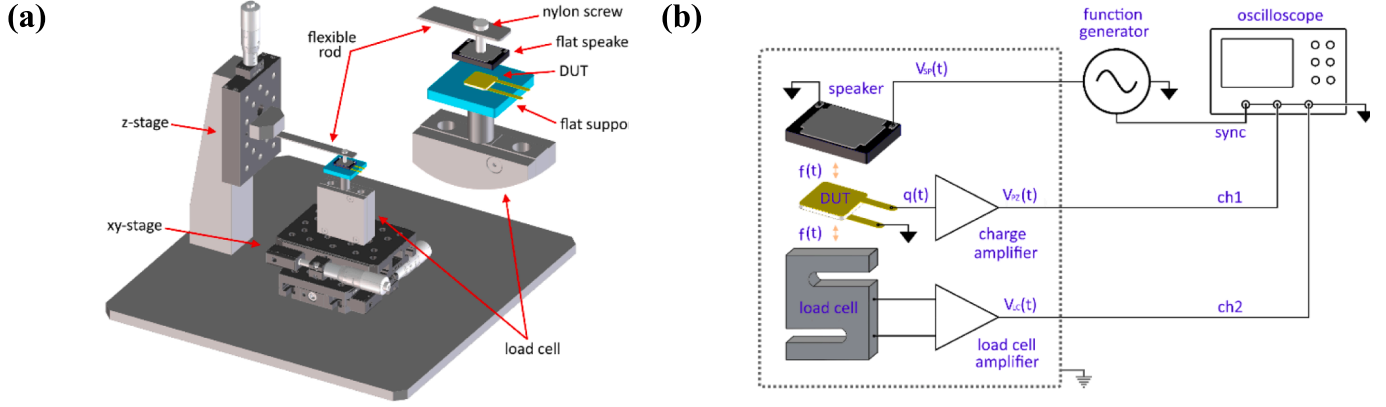
(a)

(b)

Fig. 2. A) schematic of the experimental setup for d$_{33}$ evaluation, with a magnification of the measurement stack sequence shown on the top right. b) Electrical design of the setup.

dynamic excitation force generated by the speaker and acting on the sample is quasi-statically transferred to the load cell through the sample itself and the flat support. Thus, by detecting at the same time the applied dynamic force and the charge separation signal generated by the sample through the piezoelectric direct effect, the d$_{33}$ can be effectively and accurately determined.

As depicted in Fig. 2 **b**, the exciting speaker is driven by a function generator with a sinusoidal signal whose frequency was set at 80 Hz, far from the mechanical resonance frequency of the load cell. The amplitude of the driving signal is chosen according to a preliminary static calibration (described in Section 3) to obtain the desired excitation force. The output voltage signal generated by the load cell and corresponding to the applied force is amplified by a commercial amplifier. In contrast, the sample's charge signal is converted to a voltage signal and then amplified by a custom charge amplifier. Both signals are displayed and recorded by the oscilloscope in a time frame of 100 ms and averaged 64 times to increase the signal-to-noise ratio. Signal sampling at 125 k points on the oscilloscope is synchronized with the exciting signal generated by the function generator to actuate the speaker. In this way, it is possible to couple the charge recording with the speaker actuation, both recorded as voltages, and increase the measurement precision. The adopted load cell is a ULC-2 N cell (by Interface), with a maximum load of 2 N and a maximum output voltage of 2 mV when powered at 10 V. The load cell amplifier (DMA2 by Interface) has been set with an amplification factor of 20 V mV^{-1}. The charge amplifier is a small footprint and shielded custom amplifier placed close to the sample with a conversion factor of 50 mV pC^{-1}.

2.3. Piezoelectric coefficient calculations

The piezoelectric effect is due to an interplay between the pressure applied to a material and the charges consequently developed and vice versa. The direct piezoelectric effect equation can be written as:

$$d_{33} = \left[\left(\frac{q}{A'} \right) / \left(\frac{f}{A} \right) \right] = q/f \tag{1}$$

where q is the charge developed in the piezoelectric active area A' when a force f is uniformly applied to an area A, which includes the piezoelectric active area. When the stressed area is the same as the active area, they can be neglected, and the measurement of d$_{33}$ is based only on the measurement of q and f.[24].

When time-varying force is applied, equation (1) becomes:

$$q(t) = d_{33}*f(t) \tag{2}$$

where $q(t)$ is the time-varying separation charge on the material surface, whereas $f(t)$ is the time-varying normal force on that surface.

The exciting force has a time sinusoidal behavior, which determines the charge separation behavior. The sinusoidal excitation allows static pre-load excitation to be removed, taking into account only the variable load contribution. The amplified voltage of the load cell output $V_{LC}(t)$ can be expressed considering the characteristics of the load cell and the amplifier as:

$$V_{LC}(t) = B_{LC}*f(t) \tag{3}$$

where B_{LC} is the conversion factor from load cell force to voltage output signal.

Using nominal full-scale values of the selected load cell and selected amplifier yields a force conversion factor $B_{LC} = (20 \text{ V/mV} * 2 \text{ mV}) / 2 \text{ N} = 20 \text{ V N}^{-1}$.

The output of the charge amplifier $V_{PZ}(t)$ is given by design as:

$$V_{PZ}(t) = B_{PZ}*q(t) \tag{4}$$

where B_{PZ} is the conversion factor from charge separation to voltage output signal. The conversion factor for the employed charge amplifier is $B_{PZ} = 50 \text{ mV pC}^{-1}$.

By substituting in Equation (2), this yields to:

$$d_{33} = \frac{B_{LC}*V_{PZ}}{B_{PZ}*V_{LC}} = \beta \frac{V_{PZ}}{V_{LC}} \text{ or } V_{PZ} = d_{33} \frac{V_{LC}}{\beta} \tag{5}$$

where $\beta = B_{LC}/B_{PZ}$ includes both conversion factors and where V_{PZ} and V_{LC} are the amplitudes of the peak-to-peak values.

Using nominal design values, β is around 400 pC N^{-1}.

Based on these considerations, for each measured sample, values of forces and charges, calculated according to equations (3) and (4), are plotted on the X axis and the Y axis, respectively. The slope of the obtained dispersion plot represents the value of the d$_{33}$ coefficient for that specific sample.

3. Load cell calibration

Before starting the measurements, the load cell was calibrated in static conditions to correlate the output voltage signal acquired by the oscilloscope with the measured force expressed in N. Small weights, ranging from 150 mg to 1.8 g, were placed on the stage of the load cell to exert forces in a range of about 0 – 20 mN. After each weight was placed on the stage, the DC signal generated by the load cell shifted to higher values. Values are plotted on the graph in Fig. 3**a**, whose linear fitting indicates a conversion coefficient $B_{LC} = 18.0 \text{ V N}^{-1}$, corresponding to an actual measured β of 360 pC N^{-1}. Thanks to this procedure it is possible to measure the difference in terms of voltage signal when applying the known weights and correlate it to the difference in force applied by the speaker during its sinusoidal dynamic movement. Then, to evaluate the range of forces applied by the actuation system, the speaker was
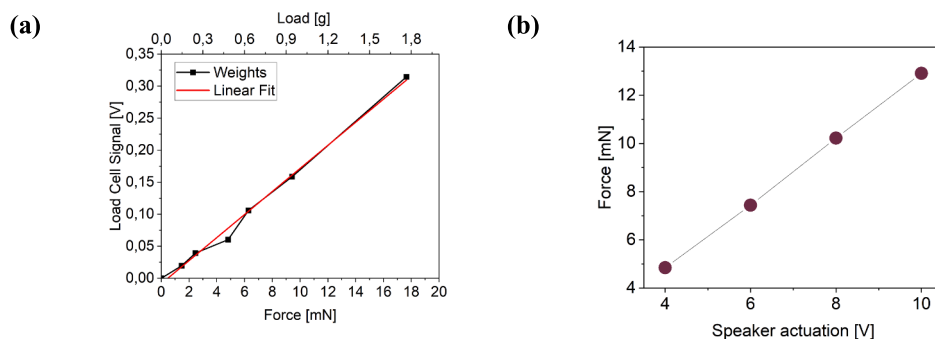
Fig. 3. A) calibration plot of the load cell. b) forces applied by the speaker as its actuation voltage increases.

positioned upside down on the load cell stage and was driven by an increasing voltage. As displayed in Fig. 3b, by increasing the voltage applied to the speaker, the displacement of the speaker rises accordingly, inducing a higher deformation to the load cell and, consequently, linearly increasing the magnitude of the applied forces (still in the range of mN to avoid sample damages).

4. Results and discussion

After calibrating the load cell, the fabricated devices were tested by the system to characterize their performance and piezoelectric features. In this respect, the PVDF sensor was enclosed in a grounded copper tape cover and placed on the load cell stage under the speaker. Then, the steel bar was adjusted in Z direction to keep all the elements in place and to apply the pre-load. After switching the speaker on, the output responses from the load cell and the charge amplifier (Fig. 4a) were acquired on the oscilloscope as voltage signals and then converted into N and pC to quantify the force and the charge, respectively. Measurements were considered valid and with impulse-free contact if the load cell signal had a sinusoidal shape following the actuation signal that drives the speaker. Indeed, when the signal is noisy or has a different shape, the mechanical contact of the elements between the steel rod and the load cell is not continuous, leading to an underestimation of the calculated coefficients. When reaching a stationary harmonic signal, it is possible to drive the speaker at different voltages to apply increasing forces to the samples. A sinusoidal fitting is applied to both signals to obtain the peak-to-peak amplitude values, which are then converted in the corresponding force and charge according to the conversion factors B_{LC} of the load cell and the conversion factor B_{PZ} of the charge amplifier. In the case of the PVDF sample, voltages from 4 to 10 V were applied to the speaker, and an increase in the peak-to-peak force signal was observed (Fig. 4 b, c). Fig. 4 d displays the trend of the peak-to-peak charge signal generated by the PVDF device. The same procedure was repeated with the AlN samples (Fig. 4 e, f and g) and with Chitosan samples (Fig. 4 h, i and j). Despite the pre-load slightly changes from one sample to another, due to small differences in the stack settings, implying a light shift of the force range applied, the magnitude remains around the tens of mN which is fairly below the yield stress of the materials measured, ensuring a non-destructive measurement. [25,26] These conditions ensure the stability of the device in time and do not alter their performances. Moreover, the force shift is accompanied by a corresponding charge shift, confirming the reliability of the measurement.

Then, a linear fitting is obtained by plotting force and charge on the X and Y axis, whose slope indicates the piezoelectric coefficient of the specific tested material (Fig. 5 a, b and c). In this respect, PVDF sample showed a d_{33} of 19 ± 1 pC N^{-1} ($R^2 = 0.99$), AlN of 6.6 ± 0.1 pC N^{-1} ($R^2 = 0.99$) and chitosan of 16 ± 2 pC N^{-1} ($R^2 = 0.93$). Indeed, the softer the material, the higher the deviation from the linear fit. It is worth noting that, although PVDF has generally a negative piezoelectric coefficient, [27,28] the commercial foil employed to fabricate the PVDF-based DUT has a positive d_{33}, as stated on its datasheet, due to a preferential orientation. However, the in-phase or out-of-phase shift between the sinusoidal charge and the force signals could give an indication whether the polarity of the studied material is positive or negative, respectively. In this case, all the three materials revealed an in-phase shift, indicating a positive-sign piezoelectric behaviour.

The measured value of d_{33} of the PVDF device is in good agreement with the $d_{33} > 18$ pC N^{-1} indicated in the material datasheet, confirming the setup's ability to measure the piezoelectric coefficient of the material correctly. Besides, standard PFM measurements of the d_{33} coefficient were used as a reference to confirm the measurements on the AlN and chitosan materials. The piezoelectric amplitude (**Fig.s 6a and d**) and phase (**Fig.s 6b and e**) on different areas in the dynamic mode were acquired for both materials. Then, spectroscopic measurements were performed on at least 5 points in the active area of each sample by applying a combination of AC (from 1 to 5 V) and DC sweep (from -10 V to 10 V) and measuring the piezoelectric expansion of the material due to the indirect piezoelectric effect (Fig. 6 c and f). The values obtained are compared to those measured on a sample with a known d_{33} to extract the piezoelectric efficiency of the materials under test. The values of the effective piezoelectric coefficients obtained are $6,0 \pm 0.1$ pm V^{-1} for the AlN sample and $15,6 \pm 0.2$ pm V^{-1} for the chitosan sample, which are in good agreement with the calculation reported previously and with literature (Table 2). These measurements prove the ability of the designed setup in assessing the d_{33} coefficient correctly.

5. Conclusions

This work proposes a method to rapidly evaluate ($\sim$ minutes) the piezoelectric coefficient d_{33} of thin and soft piezoelectric films routinely with forces in the mN range. The simultaneous acquisition of applied forces and charges allows for precisely tracking and easily quantifying of the piezoelectric behavior. The weak forces applied by a small and flat actuator prevent any damage from occurring on the soft piezoelectric material and any strain that could alter the correct quantification of the charges generated along the z-axis. Moreover, the low stiffness pre-load system and the sinusoidal actuation exclude stresses due to impacts and enable measurement in a quasi-static linear regime, which is the most appropriate method for direct piezoelectricity quantification of soft thin films. The system was tested with different commercial and home-built piezoelectric materials, spanning from synthetic and nature-derived polymers, i.e. PVDF and chitosan, to ceramic material (AlN) with different active areas, demonstrating the extremely high versatility of the system. In conclusion, thanks to its unique combination of mechanical and electrical design, this system represents a powerful instrument to evaluate the performances of thin piezoelectric film in a fast, non-destructive, accurate, and easy-to-handle way, improving the crosstalk between the optimization of the material and the design of the final device and boosting the research on new soft and flexible piezoelectric materials for wearable MEMS and health applications.
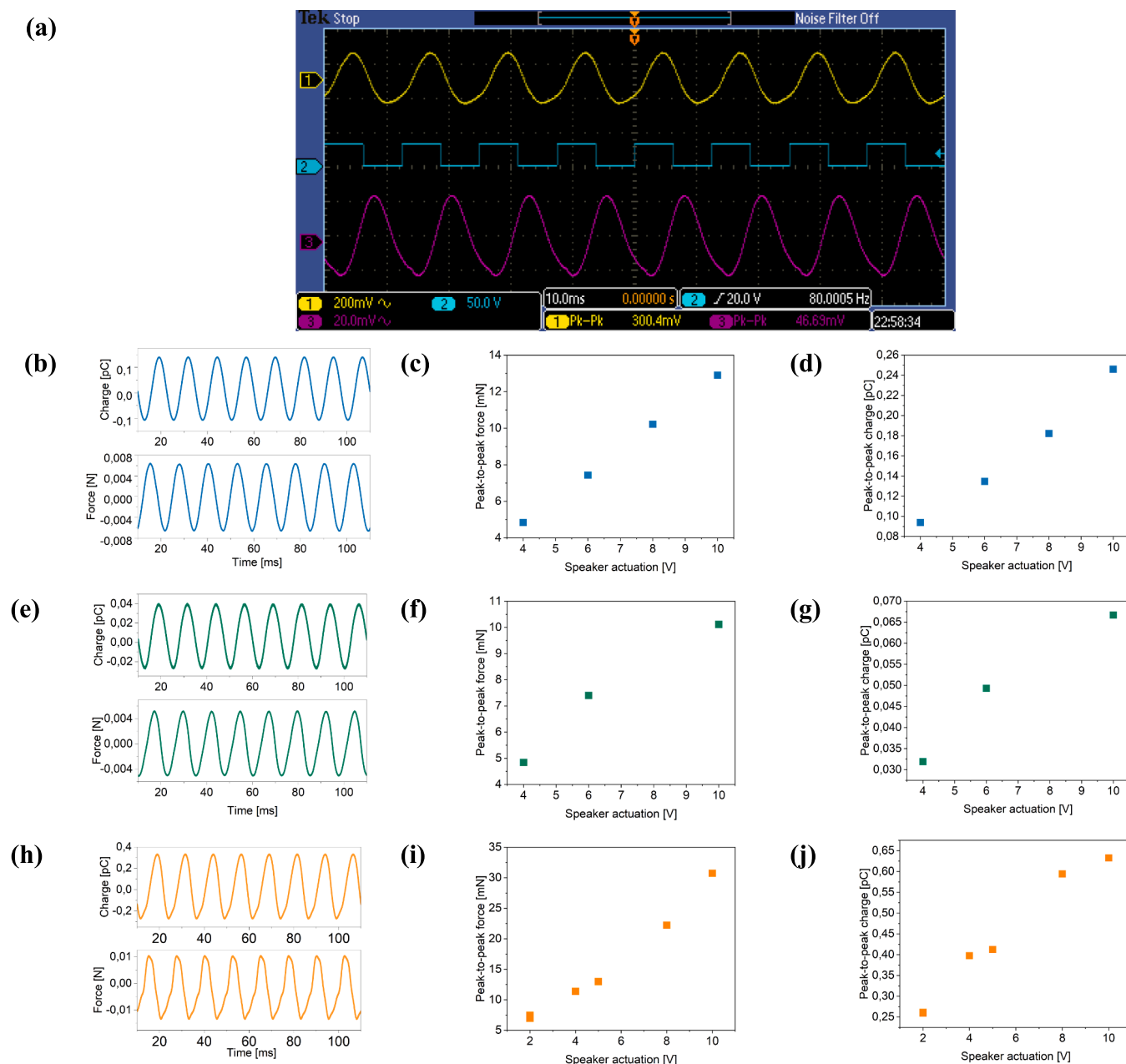
Fig. 4. A) oscilloscope display image simultaneously showing the load cell signal (yellow), the charge signal (pink) and the trigger (blue) 64 times averaged; b) signals of force and charge generated by the PVDF sensor by actuating the speaker at 10 V; c) Signals of the increasing force applied on the PVDF sample; d) Signals of the increasing charge generated by the PVDF sample during the applications of the forces in Fig. 4c; e) Signals of force and charge generated by the AlN sensor by actuating the speaker at 10 V; f) Signals of the increasing force applied on the AlN sample; g) Signals of the increasing charge generated by the AlN sample during the applications of the forces in Fig. 4f; h) Signals of force and charge generated by the chitosan sensor by actuating the speaker at 10 V; i) Signals of the increasing force applied on the chitosan sample; j) Signals of the increasing charge generated by the chitosan sample during the applications of the forces in Fig. 4i.

CRediT authorship contribution statement

Gaia de Marzo: Writing – review & editing, Writing – original draft, Software, Methodology, Investigation, Formal analysis, Data curation, Conceptualization. **Luca Fachechi:** Writing – review & editing, Writing – original draft, Software, Methodology, Investigation, Formal analysis, Data curation, Conceptualization. **Valentina Antonaci:** Investigation, Formal analysis, Data curation. **Vincenzo Mariano Mastronardi:** Writing – review & editing, Validation, Methodology. **Luigi Portaluri:** Writing – review & editing, Resources. **Maria Teresa Todaro:** Writing – review & editing, Methodology, Conceptualization. **Luciana Algieri:** Writing – review & editing, Resources. **Antonio Qualtieri:** Writing –

review & editing, Validation, Resources, Methodology. **Francesco Rizzi:** Writing – review & editing, Validation, Formal analysis. **Michele Scaraggi:** Writing – review & editing, Validation, Methodology, Formal analysis, Conceptualization. **Massimo De Vittorio:** Writing – review & editing, Validation, Supervision, Resources, Project administration, Methodology.

Declaration of competing interest

The authors declare that they have no known competing financial interests or personal relationships that could have appeared to influence the work reported in this paper.
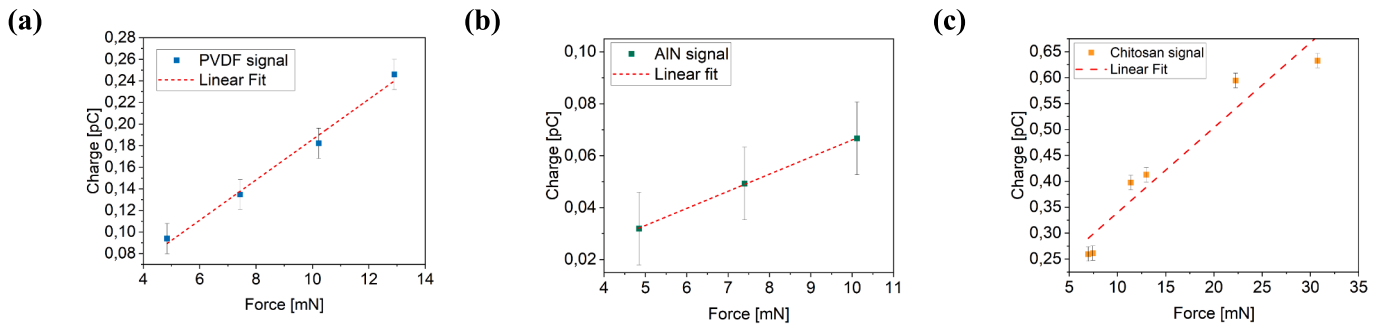
Fig. 5. A) plot of force and charge and d_{33} extrapolation for the a) PVDF, b) AlN and c) chitosan devices.
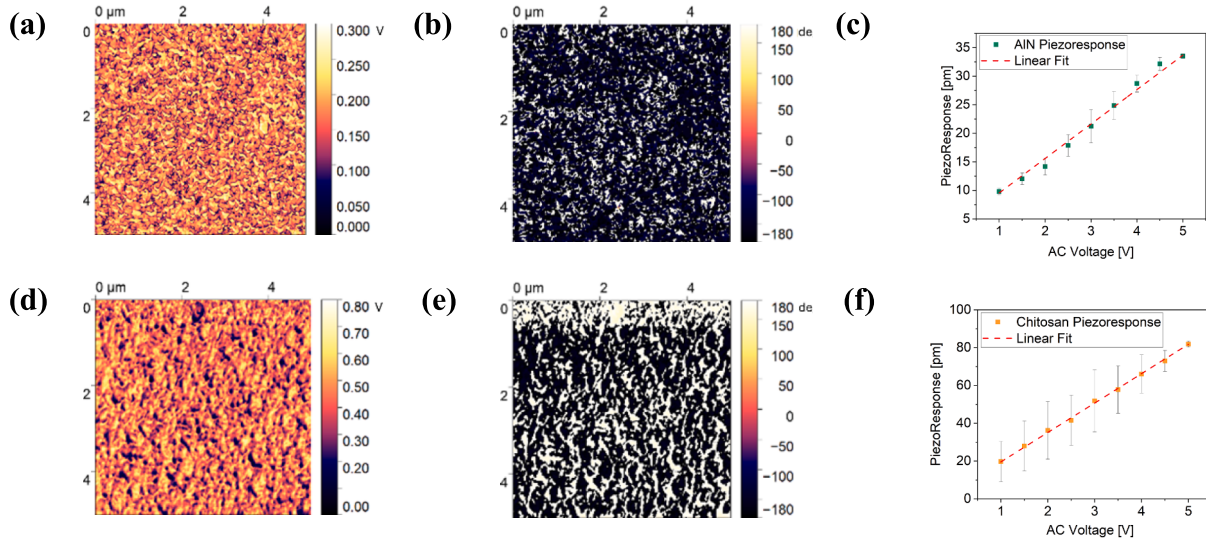

Fig. 6. A) PFM amplitude of AlN sample. b) PFM phase of AlN sample. c) average piezoresponse of AlN sample versus the AC voltage applied and fit for d_{33}^{eff} extrapolation. d) PFM amplitude of chitosan sample. e) PFM phase of chitosan sample. f) Average piezoresponse of chitosan sample versus the AC voltage applied and fit for d_{33}^{eff} extrapolation.

Table 2

Comparison of the d_{33} measured by the setup, by PFM and values reported in literature or on their datasheet.

Material	d_{33} measured with the proposed setup (pC/N)	d_{33} measured with PFM (pm/V)	d_{33}^{eff} from datasheet/ literature	reference
PVDF	19 ± 1	–	> 18 pC/N	PolyK datasheet
AlN	6.6 ± 0.1	$6,0 \pm 0.1$	$6,0 \pm 0.1$	[29]
Chitosan	16 ± 2	$15,6 \pm 0.2$	15.56 pC/N	[23]

Data availability

The data that support the findings of this study are available from the corresponding authors upon reasonable request.

References

[1] Y. Wu, Y. Ma, H. Zheng, S. Ramakrishna, Piezoelectric materials for flexible and wearable electronics: A review, Mater. Des. (2021) 110164, https://doi.org/10.1016/j.matdes.2021.110164.

[2] L. Natta, F. Guido, L. Algieri, V.M. Mastronardi, F. Rizzi, E. Scarpa, A. Qualtieri, M. T. Todaro, V. Sallustio, M. De Vittorio, Conformable AlN Piezoelectric Sensors as a Non-invasive Approach for Swallowing Disorder Assessment, ACS Sensors (2021), https://doi.org/10.1021/acssensors.0c02339.

[3] A.T. Shumba, S.M. Demir, V.M. Mastronardi, F. Rizzi, G. de Marzo, L. Fachechi, P. M. Ros, D. Demarchi, L. Patrono, M. De Vittorio, Monitoring Cardiovascular Physiology Using Bio-Compatible AlN Piezoelectric Skin Sensors, IEEE Access (2024) 16951–16962, https://doi.org/10.1109/ACCESS.2024.3359058.

[4] V. Carluccio, L. Fachechi, V.M. Mastronardi, L. Natta, L. Algieri, G. de Marzo, F. Rizzi, M. De Vittorio, Fabrication, Characterization, and Signal Processing Optimization of Flexible and Wearable Piezoelectric Tactile Sensors, IEEE Sens. J. 23 (2023) 10959–10969, https://doi.org/10.1109/JSEN.2023.3265871.

[5] R. De Fazio, V.M. Mastronardi, M. Petruzzi, M. De Vittorio, P. Visconti, Human-Machine Interaction through Advanced Haptic Sensors: A Piezoelectric Sensory Glove with Edge Machine Learning for Gesture and Object Recognition, Futur. Internet 15 (2023), https://doi.org/10.3390/fi15010014.

[6] G. de Marzo, V.M. Mastronardi, M.T. Todaro, L. Blasi, V. Antonaci, L. Algieri, M. Scaraggi, M. De Vittorio, Sustainable electronic biomaterials for body-compliant devices: Challenges and perspectives for wearable bio-mechanical sensors and body energy harvesters, Nano Energy (2024) 109336. 10.1016/j.nanoen.2024.109336.

[7] Y. Kim, J. Lee, H. Hong, S. Park, W. Ryu, Self-Powered Wearable Micropyramid Piezoelectric FilmSensor for Real-Time Monitoring of Blood Pressure, Adv. Eng. Mater. (2023), https://doi.org/10.1002/adem.202200873.

[8] T. Huang, S. Yang, P. He, J. Sun, S. Zhang, D. Li, Y. Meng, J. Zhou, H. Tang, J. Liang, G. Ding, X. Xie, Phase-Separation-Induced PVDF/Graphene Coating on Fabrics toward Flexible Piezoelectric Sensors, ACS Appl. Mater. Interfaces 10 (2018) 30732–30740, https://doi.org/10.1021/acsami.8b10552.

[9] X. Luo, Q. Li, Y. Wang, Piezoelectric Applications of Low-Dimensional Composites and Porous Materials, Materials (basel). 17 (2024), https://doi.org/10.3390/ma17040844.

[10] J. Fialka, P. Beneš, Comparison of methods of piezoelectric coefficient measurement, IEEE Trans. Instrum. Meas. (2012) 37–42, https://doi.org/10.1109/I2MTC.2012.6229293.

[11] G.J.T. Leighton, Z. Huang, Accurate measurement of the piezoelectric coefficient of thin films by eliminating the substrate bending effect using spatial scanning laser vibrometry, Smart Mater. Struct. 19 (2010), https://doi.org/10.1088/0964-1726/19/6/065011.

[12] Z. Huang, Q. Zhang, S. Corkovic, R. Dorey, R.W. Whatmore, Comparative measurements of piezoelectric coefficient of PZT films by berlincourt, interferometer, and vibrometer methods, IEEE Trans. Ultrason. Ferroelectr. Freq. Control 53 (2006) 2287–2292, https://doi.org/10.1109/TUFFC.2006.175.

[13] E. Soergel, Piezoresponse force microscopy (PFM), J. Phys. D Appl. Phys. (2011), https://doi.org/10.1088/0022-3727/44/46/464003.

[14] J. Li, J. Li, Q. Yu, Q. Nataly, S. Xie, Strain-based scanning probe microscopies for functional materials, biological structures, and electrochemical systems, J Mater. (2015), https://doi.org/10.1016/j.jmat.2015.03.001.

[15] S. Hong, Single frequency vertical piezoresponse force microscopy, J. Appl. Phys. (2021), https://doi.org/10.1063/5.0038744.

[16] B. Toroń, P. Szperlich, M. Nowak, A. Starczewska, A novel method for measuring piezoelectric coefficients, Meas. J. Int. Meas. Confed. (2023), https://doi.org/10.1016/j.measurement.2022.112274.

[17] W.W. Chen, Z.L. An, L.B. He, Z. Deng, Piezoelectric coefficients measurement for PVDF films with pneumatic pressure rig in a sole cavity, Proc. 2015 Symp.

[18] C. Ravikumar, V. Markevicius, Development of Ultrasound Piezoelectric Transducer-Based Measurement of the Piezoelectric Coefficient and Comparison with Existing Methods, Processes 11 (2023), https://doi.org/10.3390/pr11082432.

[19] I. Babu, N. Meis, G. De With, Measuring the direct piezoelectric charge coefficient for polymer matrix composites, Polym. Test. 40 (2014) 286–289, https://doi.org/10.1016/j.polymertesting.2014.10.001.

[20] Q. Guo, G.Z. Cao, I.Y. Shen, Measurements of piezoelectric coefficient d33 of lead zirconate titanate thin films using a mini force hammer, J. Vib. Acoust. Trans. ASME 135 (2013) 1–9, https://doi.org/10.1115/1.4006881.

[21] A. Šutka, P.C. Sherrell, N.A. Shepelin, L. Lapčinskis, K. Mālnieks, A.V. Ellis, Measuring Piezoelectric Output—Fact or Friction? Adv. Mater. 32 (2020) 1–9, https://doi.org/10.1002/adma.202002979.

[22] F. Guido, A. Qualtieri, L. Algieri, E.D. Lemma, M. De Vittorio, M.T. Todaro, AlN-based flexible piezoelectric skin for energy harvesting from human motion, Microelectron. Eng. (2016) 174–178, https://doi.org/10.1016/j.mee.2016.03.041.

[23] G. de Marzo, V.M. Mastronardi, L. Algieri, F. Vergari, F. Pisano, L. Fachechi, S. Marras, L. Natta, B. Spagnolo, V. Brunetti, F. Rizzi, F. Pisanello, M. De Vittorio, Sustainable, Flexible, and Biocompatible Enhanced Piezoelectric Chitosan Thin Film for Compliant Piezosensors for Human Health, Adv. Electron. Mater. 9 (2023), https://doi.org/10.1002/aelm.202200069.

[24] M. Stewart, M.G. Cain, Direct Piezoelectric Measurement: the Berlincourt Method (2014), https://doi.org/10.1007/978-1-4020-9311-1_3.

[25] S. De Bartolo, M. De Vittorio, A. Francone, F. Guido, E. Leone, V.M. Mastronardi, A. Notaro, G.R. Tomasicchio, Direct scaling of measure on vortex shedding through a flapping flag device in the open channel around a cylinder at re ~ 103: Taylor's law approach, Sensors 21 (2021) 1–18, https://doi.org/10.3390/s21051871.

[26] R. Clark, B. Averbach, The Mechanical Properties of Chitosan Membranes, Ocean. '78 (1978) 82–86.

[27] I. Katsouras, K. Asadi, M. Li, T.B. Van Driel, K.S. Kjær, D. Zhao, T. Lenz, Y. Gu, P.W. M. Blom, D. Damjanovic, M.M. Nielsen, D.M. De Leeuw, The negative piezoelectric effect of the ferroelectric polymer poly(vinylidene fluoride), Nat. Mater. 15 (2016) 78–84, https://doi.org/10.1038/nmat4423.

[28] S. Im, S.D. Bu, C. Kyu, Perspective on Ferroelectric Polymers Presenting Negative Longitudinal Piezoelectric Coefficient and Morphotropic Phase Boundary, J. Korean Inst. Electr. Electron. Mater. Eng. 35 (2022) 523–546, https://doi.org/10.4313/JKEM.2022.35.6.1.

[29] Y. Lu, M. Reusch, N. Kurz, A. Ding, T. Christoph, L. Kirste, V. Lebedev, A. Žukauskaitè, Surface Morphology and Microstructure of Pulsed DC Magnetron Sputtered Piezoelectric AlN and AlScN Thin Films, Phys. Status Solidi Appl. Mater. Sci. 215 (2018) 1–6.